

Fluorescent Sensors for Zn²⁺ Based on a Fluorescein Platform: Synthesis, Properties and Intracellular Distribution

Shawn C. Burdette,[§] Grant K. Walkup,[†] Bernhard Spingler,[§] Roger Y. Tsien,^{†,‡} and Stephen J. Lippard^{*,§}

Contribution from the Department of Chemistry, Massachusetts Institute of Technology, Cambridge, Massachusetts, 02139, and the Department of Pharmacology and Howard Hughes Medical Institute, University of California at San Diego, La Jolla, California 92093-0647

Received January 5, 2001

Abstract: Two new fluorescent sensors for Zn²⁺ that utilize fluorescein as a reporting group, Zinpyr-1 and Zinpyr-2, have been synthesized and characterized. Zinpyr-1 is prepared in one step via a Mannich reaction, and Zinpyr-2 is obtained in a multistep synthesis that utilizes 4',5'-fluorescein dicarboxaldehyde as a key intermediate. Both Zinpyr sensors have excitation and emission wavelengths in the visible range (~500 nm), dissociation constants (K_{d1}) for Zn²⁺ of <1 nM, quantum yields approaching unity ($\Phi = \sim 0.9$), and cell permeability, making them well-suited for intracellular applications. A 3- to 5-fold fluorescent enhancement is observed under simulated physiological conditions corresponding to the binding of the Zn²⁺ cation to the sensor, which inhibits a photoinduced electron transfer (PET) quenching pathway. The X-ray crystal structure of a 2:1 Zn²⁺:Zinpyr-1 complex has also been solved, and is the first structurally characterized example of a complex of fluorescein substituted with metal binding ligands.

Introduction

Zinc is a vital component in many cellular processes.¹ Although traditionally the study of Zn²⁺ bioinorganic chemistry has focused on its structural role and catalytic functions in proteins,² the neurobiology of Zn²⁺ has been a subject of increasing attention.^{3,4} Whereas most Zn²⁺ in biological systems is tightly bound in proteins, a pool of free Zn²⁺ has been imaged in cells. Included are subnanomolar concentrations in undifferentiated mammalian cells⁵ and higher concentrations, approaching 300 μ M, in the mossy fiber terminals of the hippocampus.^{6,7} The Zn²⁺ ion has the ability to modulate a variety of ion channels,⁸ may play a role in neuronal death during seizures,⁹ is pertinent to neurodegenerative disorders,¹⁰ and may be vital to neurotransmission.^{1,10} Because of these diverse functions, Zn²⁺ continues to be an interesting subject of research in neurobiology.

The levels of Zn²⁺ in the brain and other parts of the body are regulated by at least three homologous Zn²⁺ transport proteins (ZnT-1, ZnT-2, and ZnT-3)^{11–13} and by metallothio-

neins (MTs),^{14–16} including MT-III and MT-IV which are expressed mainly in the brain.^{17–20} ZnTs and MTs are probably responsible for distributing the required amounts of Zn²⁺ to proteins and enzymes, minimizing the amounts of free and potentially toxic levels of Zn²⁺ present in cells. In addition to protein regulators, Zn²⁺ can be released from synaptic vesicles^{6,21} and can enter cells through voltage-dependent Ca²⁺ channels,²² indicating that free Zn²⁺ is still available for neurological functions. Despite much research, many aspects of ionic Zn²⁺ in neurobiology remain unclear because of the limited detection methods currently available to the neuroscience community.

Fluorescent sensors are indispensable tools for visualizing ions at the molecular level without the need for special instrumentation.²³ Practical fluorescent sensors must produce a perceptible luminescent signal upon the selective binding of the desired analyte. Careful engineering of the molecular properties

(11) Palmiter, R. D.; Findley, S. D. *EMBO J.* **1995**, *14*, 639–649.

(12) Palmiter, R. D.; Cole, T. B.; Findley, S. D. *EMBO J.* **1996**, *15*, 1784–1791.

(13) Palmiter, R. D.; Cole, T. B.; Quaipe, C. J.; Findley, S. D. *Proc. Natl. Acad. Sci. U.S.A.* **1996**, *93*, 14934–14939.

(14) Ebadi, M. *Methods Enzymol.* **1991**, *205*, 363–387.

(15) Ebadi, M.; Iverson, P. L.; Hao, R.; Cerutis, D. R.; Rojas, P.; Happe, H. K.; Murrin, L. C.; Pfeiffer, R. F. *Neurochem. Int.* **1995**, *27*, 1–22.

(16) Ebadi, M.; Perini, F.; Mountjoy, K.; Garvey, J. S. *J. Neurochem.* **1996**, *66*, 2121–2127.

(17) Palmiter, R. D.; Findley, S. D.; Whitmore, T. E.; Durnam, D. M. *Proc. Natl. Acad. Sci. U.S.A.* **1992**, *89*, 6333–6337.

(18) Pountney, D. L.; Fundel, S. M.; Faller, P.; Birchler, N. E.; Hunziker, P.; Vasak, M. *FEBS Lett.* **1994**, *345*, 193–197.

(19) Tsuji, S.; Kobayashi, H.; Uchida, Y.; Ihara, Y.; Miyatake, T. *EMBO J.* **1992**, *11*, 4843–4850.

(20) Uchida, Y.; Takio, K.; Titani, K.; Ihara, Y.; Tomonaga, M. *Neuron* **1991**, *7*, 337–347.

(21) Slomianka, L. *Neuroscience* **1992**, *48*, 325–352.

(22) Atar, D.; Backx, P. H.; Appel, M. M.; Gao, W. D.; Marban, E. *J. Biol. Chem.* **1995**, *270*, 2473–2477.

(23) de Silva, A. P.; Gunaratne, H. Q. N.; Gunnlaugsson, T.; Huxley, A. J.; McCoy, C. P.; Rademacher, J. T.; Rice, T. E. *Chem. Rev.* **1997**, *97*, 1515–1566.

[§] Massachusetts Institute of Technology.

[†] Department of Pharmacology, University of California at San Diego.

[‡] Howard Hughes Medical Institute, University of California at San Diego.

(1) Vallee, B. L.; Falchuk, K. H. *Physiol. Rev.* **1993**, *73*, 79–118.

(2) Lippard, S. J.; Berg, J. M. *Principles of Bioinorganic Chemistry*; University Science Books: Mill Valley, 1994.

(3) Frederickson, C. J. *Int. Rev. Neurobiol.* **1989**, *31*, 145–238.

(4) Huang, E. P. *Proc. Natl. Acad. Sci. U.S.A.* **1997**, *94*, 13386–13387.

(5) Nasir, M. S.; Fahrni, C. J.; Suhy, D. A.; Kolodnick, K. J.; Singer, C. P.; O'Halloran, T. V. *J. Biol. Inorg. Chem.* **1999**, *4*, 775–783.

(6) Frederickson, C. J.; Moncrieff, D. W. *Biol. Signals* **1994**, *3*, 127–139.

(7) Budde, T.; Minta, A.; White, J. A.; Kay, A. R. *Neuroscience* **1997**, *79*, 347–358.

(8) Harrison, N. L.; Gibbons, S. J. *Neuropharmacology* **1994**, *33*, 935–952.

(9) Choi, D. W.; Koh, J. Y. *Annu. Rev. Neurosci.* **1998**, *21*, 347–375.

(10) Cuajungco, M. P.; Lees, G. J. *Neurobiol. Dis.* **1997**, *4*, 137–169.

of these probes can provide an effective methodology for studying relevant intracellular metal ions, such as Ca^{2+} in biological systems.²⁴ In addition to selectivity for the analyte, biosensors should have a K_d value near the median concentration of the species under investigation to allow concentration changes to be monitored. Desirable intracellular fluorescent sensors should produce a signal with a high quantum yield (Φ) and have excitation wavelengths exceeding 340 nm. The latter property permits use with glass microscope objectives and prevents UV-induced cell damage. A good sensor will also have emission wavelengths approaching 500 nm to avoid autofluorescence from species native to the cell and to facilitate use with typical fluorescence microscopy optical filter sets.²⁵ Finally, sensors must have the ability to be passively and irreversibly loaded into cells.

The majority of studies of intracellular Zn^{2+} with fluorescent sensors have been performed with TSQ,²⁶ Zinquin,^{27,28} and TFLZn,⁷ all of which are aryl sulfonamide derivatives of 8-aminoquinoline. Recent investigations into the aqueous binding properties of these compounds have clarified many discrepancies found in the literature on these probes, promoting the accuracy of results for future application of these sensors.^{5,29} Although quinoline-based probes are useful, these sensors are not ideal, because they require near-ultraviolet excitation and can form mixed complexes sensing partially coordinated Zn^{2+} . Several approaches to fluorescent Zn^{2+} detection based on polypeptide,^{30–32} protein,³³ and macrocyclic^{34–36} sensors have been reported, but none has been applied successfully to sensing zinc in living cells. These alternative sensors are not suitable for intracellular work because of either unsatisfactory binding affinity, optical properties, and cell toxicity, or the need to perform microinjections into cells. Several traditional Ca^{2+} and Mg^{2+} probes have been utilized to study Zn^{2+} ,^{22,37} but results from these applications can be ambiguous, because Zn^{2+} -induced signals are difficult to distinguish from those involving alkaline earth metal ions. Recently, the synthesis and characterization of ZnAF-1 and ZnAF-2, two aminofluorescein-based Zn^{2+} sensors, were reported.³⁸ The esterified forms of these new sensors are cell-permeable, but details about their intracellular behavior were not described.

In an effort to facilitate the understanding of Zn^{2+} in cell biology and neurology, we recently described the preparation

(24) Tsien, R. Y. *Fluorescent and Photochemical Probes of Dynamic Biochemical Signals Inside Living Cells*; Czarnik, A. W., Ed.; American Chemical Society: Washington D. C., 1993; Vol. 538, pp 130–146.

(25) Czarnik, A. W. *Curr. Biol.* **1995**, *2*, 423–428.

(26) Frederickson, C. J.; Kasarskis, E. J.; Ringo, D.; Frederickson, R. E. *J. Neurosci. Methods* **1987**, *20*, 91–103.

(27) Zalewski, P. D.; Forbes, I. J.; Betts, W. H. *Biochem. J.* **1993**, *296*, 403–408.

(28) Mahadevan, I. B.; Kimber, M. C.; Lincoln, S. F.; Tiekink, E. R. T.; Ward, A. D.; Betts, W. H.; Forbes, I. J.; Zalewski, P. D. *Aust. J. Chem.* **1996**, *49*, 561–568.

(29) Fahrni, C. J.; O'Halloran, T. V. *J. Am. Chem. Soc.* **1999**, *121*, 11448–11458.

(30) Godwin, H. A.; Berg, J. M. *J. Am. Chem. Soc.* **1996**, *118*, 6514–6515.

(31) Walkup, G. K.; Imperiali, B. *J. Am. Chem. Soc.* **1997**, *119*, 3443–3450.

(32) Walkup, G. K.; Imperiali, B. *J. Org. Chem.* **1998**, *63*, 6727–6731.

(33) Thompson, R. B.; Maliwal, B. P.; Fierke, C. A. *Anal. Chem.* **1998**, *70*, 1749–1754.

(34) Czarnik, A. W. *Acc. Chem. Res.* **1994**, *27*, 302–308.

(35) Koike, T.; Watanabe, T.; Aoki, S.; Kimura, E.; Shiro, M. *J. Am. Chem. Soc.* **1996**, *118*, 12696–12703.

(36) Hirano, T.; Kikuchi, K.; Urano, Y.; Higuchi, T.; Nagano, T. *Angew. Chem., Int. Ed.* **2000**, *39*, 1052–1054.

(37) Canzoniero, L. M. T.; Sensi, S. L.; Choi, D. W. *Neurobiol. Dis.* **1997**, *4*, 275–279.

(38) Hirano, T.; Kikuchi, K.; Urano, Y.; Higuchi, T.; Nagano, T. *J. Am. Chem. Soc.* **2000**, *122*, 12399–12400.

and preliminary characterization of Zinpyr-1,³⁹ a new cell-permeable fluorescent sensor for Zn^{2+} .⁴⁰ Our initial investigations indicated that Zinpyr-1 exhibits a 3.1-fold increase in integrated fluorescence intensity upon the formation of a 1:1 ligand: Zn^{2+} complex. Zinpyr-1 can be passively loaded into cells and used to detect Zn^{2+} introduced exogenously. Zinpyr-1 is particularly amenable to intracellular work, because fluorescein is the reporting group. This xanthenone-based chromophore has a quantum yield approaching unity ($\Phi = 0.95$) and excitation and emission wavelengths exceeding 490 nm.⁴¹

Previous approaches to preparing fluorescent sensors have often suffered from a lack of generality. We have therefore devised a general methodology for preparing fluorescent sensors that is based on the fluorescein framework and demonstrate here its utility through the synthesis of Zinpyr-2, a first-generation fluorescent probe structurally similar to Zinpyr-1. In addition, we describe a thorough investigation of the physical and structural properties of these probes related to their use as Zn^{2+} sensors.

Experimental Section

Materials and Methods. Chlorobenzene and 1,2-dichloroethane (DCE) were distilled from calcium hydride under nitrogen. Dimethyl sulfoxide (DMSO) was vacuum distilled from CaH_2 and subsequently dried over 3-Å molecular sieves. Deuterated chloroform was dried over 3-Å molecular sieves. Zinc chloride was fused prior to each use. Di-(2-picoly)amine (DPA) was prepared as previously described.⁴² All other reagents were purchased and used as received. Flash column chromatography was performed using silica gel-60 (230–400 mesh) or Brockman I activated neutral aluminum oxide (150 mesh). Thin-layer chromatography (TLC) analysis was performed using Merck F254 silica gel-60 plates or Merck F254 aluminum oxide-60 and viewed by UV light, or developed with ceric ammonium molybdate, 2,4-dinitrophenyl hydrazine, or iodine stain. Infrared spectra were recorded on a BTS 135 FTIR instrument as KBr pellets. NMR spectra were recorded on a Varian 500 MHz spectrometer at ambient probe temperature, 283 K, and were referenced to the internal ^1H and ^{13}C solvent peaks. Fast atom bombardment (FAB) mass spectrometry was performed in the MIT Department of Chemistry Instrumentation Facility (DCIF) with the use of *m*-nitrobenzyl alcohol as the matrix. Melting points were recorded on a Thomas–Hoover capillary melting point apparatus. **CAUTION: One of the isolated compounds below contains perchlorate ion, which can detonate explosively and without warning. Although we have encountered no incidents with the reported compound, all due precautions should be taken.**

4',5'-Dimethylfluorescein Dibenzoate (1). Phthalic anhydride (16.7 g, 113 mmol) and 2-methylresorcinol (24.9 g, 201 mmol) were crushed and melted into a brown liquid at 150 °C. Fused ZnCl_2 (15 g, 110 mmol) was added slowly over 35 min, and the temperature was slowly increased to 230 °C over 30 min until the material solidified. The brick red solid was pulverized and boiled in 250 mL of 6 M HCl for 30 min. The red solid was collected on a frit, washed thoroughly with distilled water, and dried in vacuo at 50 °C for 2 h. The crude product was combined with benzoic anhydride (115 g, 509 mmol) in 400 mL of pyridine and refluxed at 140 °C for 2.5 h. The reaction mixture was diluted with 700 mL of distilled water, and a dark brown solid formed upon cooling. The solids were collected, washed thoroughly with water, and dried. The dark brown solids were dissolved in 550 mL of boiling toluene and decolorizing carbon was added. The hot mixture was filtered through Celite, and the Celite/carbon mixture was washed with 250 mL of boiling toluene. The product was crystallized from toluene and

(39) The name Zinpyr indicates the structural composition of the ligand (four pyridyl groups) as well as its ability to “peer” into the Zn^{2+} concentration of samples.

(40) Walkup, G. K.; Burdette, S. C.; Lippard, S. J.; Tsien, R. Y. *J. Am. Chem. Soc.* **2000**, *122*, 5644–5645.

(41) Lakowicz, J. R. *Principles of Fluorescence Spectroscopy*; 2nd ed.; Kluwer Academic/Plenum: New York, 1999.

(42) Gruenwedel, D. W. *Inorg. Chem.* **1968**, *7*, 495–501.

recrystallized (4:1 toluene/EtOH) to yield a white crystalline solid (32.3 g, 56.7%); TLC R_f = 0.41 (3:1 hexanes/EtOAc); mp = 240–42 °C. ¹H NMR (CDCl₃, 500 MHz) δ 2.42 (6H, s), 6.76 (2H, d, J = 9.0 Hz), 6.93 (2H, d, J = 8.5 Hz), 7.28 (1H, d, J = 7.5 Hz), 7.55 (4H, t, J = 7.5 Hz), 7.65–7.74 (4H, m), 8.06 (1H, d, J = 8.0 Hz), 8.25 (4H, d, J = 7.5 Hz). ¹³C NMR (CDCl₃, 125 MHz) δ 9.85, 82.97, 116.60, 118.09, 119.63, 124.47, 125.39, 125.79, 126.60, 128.91, 129.14, 130.16, 130.48, 134.11, 135.35, 150.44, 150.80, 153.03, 164.74, 169.42. FTIR (KBr, cm⁻¹) 1771, 1763, 1738, 1599, 1592, 1452, 1421, 1267, 1222, 1099. HRMS (+FAB) calcd for MH⁺, 569.1600; found, 569.1588.

4',5'-Bis(bromomethyl)fluorescein Dibenzoate (2), 4',5'-Dimethylfluorescein dibenzoate (5.00 g, 8.79 mmol) and 1,3-dibromo-5,5-dimethylhydantoin (3.87 g, 13.6 mmol) were combined in 550 mL of C₆H₅Cl, and acetic acid (133 μ L, 2.32 μ mol) and 1,1'-azobis(cyclohexanecarbonitrile) (0.181 g, 0.740 mmol) were added to the solution with stirring. The solution was stirred at 40 °C for 72 h and then washed four times with hot water (100 mL, 80 °C). Recrystallization (9:1 toluene:EtOH) and washing with *n*-pentane yielded the product as a white crystalline solid (6.27 g, 98.2%). TLC R_f = 0.34 (7:3 hexanes:EtOAc); mp = 300 °C dec. ¹H NMR (CDCl₃, 500 MHz) δ 4.87 (2H, d, J = 10.0 Hz), 4.88 (2H, d, J = 10.5 Hz), 6.92 (2H, d, J = 8.5 Hz), 7.08 (2H, d, J = 9.0 Hz), 7.32 (1H, d, J = 8.0 Hz), 7.58 (4H, t, J = 7.5 Hz), 7.68–7.78 (4H, m), 8.08 (1H, d, J = 8.5 Hz), 8.28 (4H, d, J = 7.0 Hz). ¹³C NMR (CDCl₃, 125 MHz) δ 20.69, 81.60, 117.09, 119.21, 119.38, 124.47, 125.63, 126.36, 128.68, 128.99, 129.10, 130.58, 130.65, 134.50, 135.71, 149.63, 150.79, 152.48, 164.39, 169.04. FTIR (KBr, cm⁻¹) 1774, 1743, 1601, 1589, 1427, 1234, 1081, 1066. HRMS (+FAB) calcd for MH⁺, 724.9811; found, 724.9824.

4',5'-Fluoresceindicarboxaldehyde (3), 4',5'-Bis(bromomethyl)fluorescein dibenzoate (2.00 g, 2.75 mmol) and NaHCO₃ (2.00 g, 23.8 mmol) were combined in 200 mL of DMSO and heated to 150 °C for 4 h. The dark red solution was cooled and then diluted into 700 mL of 2 M HCl and stirred for 2 h. The aqueous material was extracted thoroughly with CH₂Cl₂ (8 \times 100 mL), and the solvents were removed to isolate an orange liquid. The orange solid that precipitated with the addition of 300 mL of water was collected on a frit and washed thoroughly with water. The orange solid was redissolved in CH₂Cl₂ and dried over Na₂SO₄. An orange solid was isolated after filtration and solvent removal. Flash chromatography on silica gel (33:1 CHCl₃:MeOH) yielded the product as a yellow powder (391 mg, 36.7%). TLC R_f = 0.46 (19:1 CHCl₃:CH₃OH); mp = 301–303 °C dec. ¹H NMR (CDCl₃, 500 MHz) δ 6.74 (2H, d, J = 8.5 Hz), 6.94 (2H, d, J = 9.5 Hz), 7.18 (1H, d, J = 7.5 Hz), 7.69 (1H, td, J = 1.0, 7.5 Hz), 7.74 (1H, td, J = 1.0, 7.5 Hz), 8.07 (1H, d, J = 7.5 Hz), 10.67 (2H, s), 12.13 (2H, s). ¹³C NMR (CDCl₃, 125 MHz) δ 80.80, 109.23, 109.71, 115.42, 123.90, 125.76, 126.73, 130.72, 135.86, 137.16, 151.87, 152.11, 164.87, 168.87, 192.00. FTIR (KBr, cm⁻¹) 1769, 1656, 1600, 1228, 1172, 1092. HRMS (+FAB) calcd for MH⁺, 389.0661; found, 389.0674.

9-(*o*-Carboxyphenyl)-4,5-bis[bis(2-pyridylmethyl)aminomethyl]-6-hydroxy-3-xanthanone (Zinpyr-2, 4), 4',5'-Fluorescein-dicarboxaldehyde (200 mg, 0.515 mmol) and acetic acid (120 μ L, 2.1 mmol) were combined in 1,2-dichloroethane (DCE, 30 mL) and stirred. To the resulting solution, DPA (215 mg, 1.08 mmol) in DCE (20 mL) was added dropwise and stirred for 30 min. Sodium triacetoxyborohydride (230 mg, 1.08 mmol) was added, and the reaction mixture was stirred 12 h at room temperature. The reaction was chilled to 0 °C, and water was added to the solution with stirring. The aqueous layer was extracted with CH₂Cl₂, and the combined organic layers were washed twice with saturated NaCl to give an orange solid after solvent removal. The compound was dried by azeotroping with benzene. Flash chromatography on activated neutral alumina (24:1 CHCl₃:MeOH) yielded the product as an orange solid (108 mg, 27.8%). TLC R_f = 0.10 (alumina, 19:1 CHCl₃:CH₃OH); mp = 195–197 °C dec. ¹H NMR (CDCl₃, 500 MHz) δ 3.98 (4H, d, J = 15.0 Hz), 4.02 (4H, d, J = 15.0 Hz), 4.18 (4H, s), 6.57 (2H, d, J = 8.5 Hz), 6.64 (2H, d, J = 8.5 Hz), 7.17–7.21 (5H, m), 7.37 (4H, d, J = 7.5 Hz), 7.58–7.67 (6H, m), 8.00 (1H, d, J = 7.5 Hz), 8.59 (4H, d, J = 6.5 Hz). ¹³C NMR (CDCl₃, 125 MHz) δ 49.24, 59.45, 109.84, 110.24, 113.38, 122.57, 123.52, 124.38, 125.10, 127.69, 128.30, 129.70, 134.92, 137.16, 149.02, 150.59,

152.86, 158.19, 160.21, 169.64. FTIR (KBr, cm⁻¹) 3448, 1755, 1591, 1435, 760. HRMS (+FAB) calcd for MH⁺, 755.2982; found, 755.2959.

9-(*o*-Carboxyphenyl)-2,7-dichloro-4,5-bis[bis(2-pyridylmethyl)aminomethyl]-6-hydroxy-3-xanthanone (Zinpyr-1, 5), DPA (1.59 g, 7.99 mmol) and paraformaldehyde (0.224 g, 7.47 mmol) were combined in 20 mL of CH₃CN and refluxed for 30 min. 2',7'-Dichlorofluorescein (1.00 g, 2.49 mmol) in 30 mL of CH₃CN/H₂O (1:1) was added to the solution, and the reaction mixture was refluxed for 24 h. The CH₃CN was removed, and the product and residual water were triturated with 30 mL of boiling ethanol. The product was precipitated at –25 °C, filtered on a frit, washed thoroughly with ice-cold water, and dried. Flash chromatography on activated neutral alumina (45:1 CHCl₃:MeOH) yielded the product as a salmon-pink solid (960 mg, 46.8%). TLC R_f = 0.10 (alumina, 19:1 CHCl₃:CH₃OH); mp = 185–187 °C dec. ¹H NMR (CDCl₃, 500 MHz) δ 3.98 (4H, d, J = 15.0 Hz), 4.01 (4H, d, J = 15.0 Hz), 4.20 (4H, s), 6.64 (2H, s), 7.19 (5H, t, J = 7.5 Hz), 7.36 (4H, d, J = 8.0 Hz), 7.64–7.73 (6H, m), 8.04 (1H, d, J = 7.0 Hz), 8.60 (4H, dq, J = 1.0, 5.0 Hz). ¹³C NMR (CDCl₃, 125 MHz) δ 49.38, 59.31, 89.44, 110.26, 111.93, 117.72, 122.67, 123.43, 124.27, 125.54, 127.28, 127.86, 130.31, 135.41, 137.32, 148.99, 151.83, 156.09, 157.81, 169.13. FTIR (KBr, cm⁻¹) 3447, 1761, 1750, 1592, 1475, 1435, 761. HRMS (+FAB) calcd for MH⁺, 823.2202; found, 823.2229.

[Zn₂(Zinpyr-1)(H₂O)₂](ClO₄)₂ (6), Zinpyr-1 (50.6 mg, 61.5 μ mol) was combined with zinc triflate (2.00 mL, 0.121 M, 243 μ mol) and sodium hydroxide (2.00 mL, 0.121 M, 243 μ mol) in CH₃CN (5 mL) and sonicated for 10 min to dissolve all of the solids. Sodium perchlorate (0.500 g, 4.70 mmol) was dissolved in water (5 mL) and added to the CH₃CN solution, then the combined solutions were filtered through Celite. The product partially crystallized at room temperature after 12 h. The remainder of the product was crystallized at –25 °C over 12 h. The orange crystalline material was filtered, powdered, and dried under vacuum at 50 °C to yield 37.0 mg of dried product in 48.4% yield. Analogous small-scale reactions at 25 °C yielded orange square prisms suitable for X-ray crystallography. ¹H NMR (DMSO-*d*₆, 500 MHz) δ 4.13–4.41 (12H, m), 6.14 (2H, s), 7.14 (1H, d, J = 8.0 Hz), 7.54 (4H, q, J = 8.0 Hz), 7.604 (4H, t, J = 8.0 Hz), 7.70 (1H, t, J = 7.0 Hz), 7.84 (1H, t, J = 7.5 Hz), 7.92 (1H, t, J = 7.5 Hz), 8.07 (4H, quin, J = 1.5, 7.5 Hz), 8.68 (2H, d, J = 5.0 Hz), 8.74 (2H, d, J = 5.0 Hz). FTIR (KBr, cm⁻¹) 3441, 1748, 1610, 1571, 1457, 1363, 1121. Anal. Calcd for Zn₂C₄₆H₄₀N₆O₁₆ (6•H₂O): C, 45.84; H, 3.34; N, 6.97. Found: C, 45.89; H, 3.13; N, 6.71.

Collection and Reduction of X-ray Data. Crystals were covered with Paratone-N oil and suitable specimens were mounted on the tips of glass fibers at room temperature and transferred to a Bruker (formerly Siemens) CCD X-ray diffraction system with a graphite-monochromatized Mo K α radiation (λ = 0.71073 Å) controlled by a Pentium-based PC running the SMART software package.⁴³ Data were collected at 188 K in a stream of cold N₂ maintained with a Siemens LT-2A nitrogen cryostat. Procedures for data collection and reduction have been reported previously.⁴⁴ The structure was solved by direct methods and refined by full matrix least-squares and difference Fourier techniques with SHELXTL.⁴⁵ Empirical absorption corrections were applied with the SADABS program,⁴⁶ and the structure was checked for higher symmetry by PLATON.⁴⁷ The space group was determined by examining systematic absences and confirmed by the successful solution and refinement of the structure. All non-hydrogen atoms were refined anisotropically. Hydrogen atoms were assigned idealized locations and given isotropic thermal parameters 1.2 \times the thermal parameter of the carbon atoms to which they were attached. In the structure of 6•6H₂O, one perchlorate anion is disordered and several water molecules are partially occupied; all were modeled and refined accordingly. Relevant crystallographic information is summarized in Table 1, and the 50% thermal ellipsoid plot is shown in Figure 1.

(43) SMART, 5.05 ed.; Bruker AXS, Inc.: Madison, WI, 1998.

(44) Feig, A. L.; Bautista, M. T.; Lippard, S. J. *Inorg. Chem.* **1996**, *25*, 6892–6898.

(45) Sheldrick, G. M. *SHELXL97-2: Program for the Refinement of Crystal Structures*; University of Göttingen: Germany, 1997.

(46) Sheldrick, G. M. *SADABS: Area-Detector Absorption Correction*; University of Göttingen: Germany, 1996.

(47) Spek, A. L. *PLATON, A Multipurpose Crystallographic Tool*; Utrecht University: Utrecht, The Netherlands, 1998.

Table 1. Crystallographic Parameters for $[\text{Zn}_2(\text{Zinpyr}-1)(\text{H}_2\text{O})_2](\text{ClO}_4)_2 \cdot 6\text{H}_2\text{O}$ ($6 \cdot 6\text{H}_2\text{O}$)

formula	$\text{C}_{46}\text{H}_{34}\text{Cl}_4\text{N}_6\text{O}_{21}\text{Zn}_2$
formula wt	1279.33
space group	$P2_1/n$
a , Å	14.1579(4)
b , Å	18.2353(4)
c , Å	21.7207(3)
β , deg	90.705(2)
V	5607.3(2)
Z	4
ρ_{calc} (g cm ⁻³)	1.515
absorp. coeff. (mm ⁻¹)	1.126
temp, K	188(2)
total no. data	28159
no. of unique data	9552
obs data ^a	5316
no. parameters	724
R , % ^b	8.96
wR_2 , % ^c	16.86
max/min peaks, e/Å ³	0.867, -0.496

^a Observation criterion: $I > 2\sigma(I)$. ^b $R = \sum||F_o| - |F_c||/\sum|F_o|$. ^c $wR_2 = \{\sum[w(F_o^2 - F_c^2)^2]/\sum[w(F_o^2)^2]\}^{1/2}$.

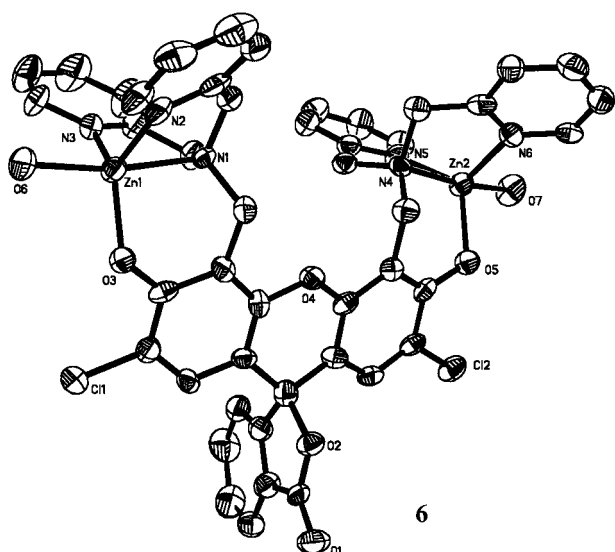


Figure 1. ORTEP diagram of $[\text{Zn}_2(\text{Zinpyr}-1)(\text{H}_2\text{O})_2](\text{ClO}_4)_2 \cdot 6\text{H}_2\text{O}$ ($6 \cdot 6\text{H}_2\text{O}$) showing 50% thermal ellipsoids and selected atom labels. Water molecules, hydrogen atoms, and disordered perchlorates are omitted for clarity.

General Spectroscopic Methods. Ultrapure grade HEPES (2[4-(2-hydroxyethyl)-1-piperazinyl]ethanesulfonic acid) and PIPES (piperazine-*N,N'*-bis(2-ethanesulfonic acid)) from Calbiochem and KCl (99.997%) were purchased and used as received. All solutions were filtered through 0.2- μm cellulose filters before measurements. Except for the fluorescence titration experiment, Zn solutions were prepared by the addition of appropriate amounts of 1.0 M, 100 mM, 10 mM or 1 mM Zn^{2+} stocks that were checked by atomic absorption spectroscopy for concentration accuracy, or by titration with terpyridine and measurement of the absorption spectra. The titration was performed by treating a 70 μM solution of 2,2':6',2''-terpyridine in 10 mM PIPES, pH 7.0, with aliquots of 10 mM (nominal) ZnCl_2 and determining the equivalence point by monitoring the absorbance of the resulting complex at 335 nm ($\epsilon = 28.5 \times 10^3 \text{ M}^{-1} \text{ cm}^{-1}$). The Zn^{2+} stocks were prepared from 99.999% pure ZnCl_2 . The purity of the Zinpyr probes was verified to be greater than 99% by HPLC. Zinpyr was introduced to aqueous solutions by addition of a stock solution in DMSO (0.67 μM). Graphs were manipulated and equations were calculated by using Kaleidagraph 3.0. The pH values of solutions were recorded using an Orion glass electrode that was calibrated prior to each use.

UV-Visible Spectroscopy. Absorption spectra were recorded on a Hewlett-Packard 8453A diode array spectrophotometer under the control

of a Pentium II-based PC running the Windows NT ChemStation software package or a Cary 1E scanning spectrophotometer under the control of a Pentium PC running the manufacturer-supplied software package. Spectra were routinely acquired at 25 °C, which was maintained by a circulating water bath in 1-cm path length quartz cuvettes having a volume of 1.0 or 3.5 mL.

Fluorescence Spectroscopy. Fluorescence spectra were recorded on a Hitachi F-3010 spectrofluorimeter under the control of a Pentium-based PC running the SpectraCalc software package. Excitation was provided by a 150 W Xe lamp (Ushio Inc.) operating at a current of 5 A. All spectra were normalized for excitation intensity via a rhodamine quantum counter, and emission spectra were normalized by the manufacturer-supplied correction curves. Spectra were routinely acquired at 25 °C, maintained by a circulating water bath in 1 cm \times 1 cm quartz cuvettes using 3 nM slit widths and a 240 nm/min scan speed. Fluorescence emission measurements were also acquired in a 1 cm \times 1 cm quartz cell using a Spex Fluorolog-2 instrument with 1-nm bandwidth slits. All spectra were corrected for emission intensity by using the manufacturer-supplied photomultiplier curves.

(a) pH-Dependent Fluorescence Studies. The apparent pK_a was measured by plotting the integrated area of the fluorescence emission spectrum against pH recorded in the range from pH 12.5 to 2.5. A 1 μM solution of the Zinpyr dye (10 mL) containing ~ 1 mM KOH and 100 mM KCl was adjusted to pH 12.5, and the UV-vis and fluorescence spectra were recorded. The pH was lowered in steps of $\Delta\text{pH} = 0.5$ with the addition of appropriate amounts of 6, 2, 0.5, 1, 0.1, and 0.01 N HCl, recording the absorption and emission spectra at each pH interval. The volume of the solution was controlled such that the overall change in volume was $< 2\%$. Emission for Zinpyr-1 was integrated from 450 to 700 nm. Emission for Zinpyr-2 was integrated from 500 to 700 nm. The resulting integrated emission spectral areas were normalized, plotted against pH, and fit to the nonlinear expression in eq 1 to calculate the pK_a value. In the equation, $\Delta F_{1\text{max}}$ and $\Delta F_{2\text{max}}$ are the maximum fluorescence changes associated with the corresponding pK_a values.

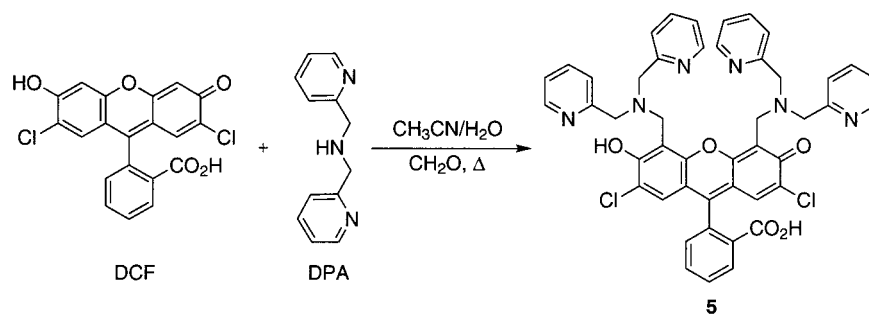
$$\Delta F = \frac{\Delta F_{1\text{max}}}{(1 + 10^{(\text{pH} - pK_{a1})})} + \frac{\Delta F_{2\text{max}}}{(1 + 10^{(\text{pH} - pK_{a2})})} \quad (1)$$

(b) Quantum Yield. The quantum yields for fluorescence were obtained by comparison of the integrated area of the corrected emission spectrum of the samples with that of a solution of fluorescein in 0.1 N NaOH, which has a quantum efficiency of 0.95.⁴¹ The concentration of the reference was adjusted to match the absorbance of the test sample. The quantum efficiency of the metal-free ligand was measured by using a dilute sample of Zinpyr dye ($\sim 1 \times 10^{-6}$ M, Abs ≤ 0.1) in 10 mM PIPES, pH = 7.0; 100 mM KCl; and 50 μM EDTA. The quantum efficiency of metal-bound ligand was measured by using a dilute sample of Zinpyr ($\sim 8 \times 10^{-7}$ M, Abs ≤ 0.1) in 10 mM PIPES, pH = 7.0; 100 mM KCl; and 100 μM ZnCl_2 . The concentration of the reference was adjusted to match the absorbance of the test sample at the wavelength of excitation. Emission for Zinpyr-1 was integrated from 480 to 650 nm with excitation at 475 nm, and emission for Zinpyr-2 was integrated from 496 to 600 nm with excitation at 492 nm. The quantum yields were calculated with the expression in eq 2.

$$\Phi_{\text{sample}} = \Phi_{\text{standard}} \times \frac{\int \text{emission}_{\text{sample}}}{\int \text{emission}_{\text{standard}}} \quad (2)$$

(c) Titration of Zn^{2+} Binding by Fluorescence Spectroscopy (K_d). The first K_d associated with Zn^{2+} binding was measured by a fluorescence titration as described previously.⁴⁸ Zinpyr-1 spectra were acquired by exciting at 507 nm and integrating the emission from 475 to 650 nm. Zinpyr-2 spectra were acquired by exciting at 490 nm and collecting and integrating data from 500 to 575 nm. The measurements were performed in triplicate to ensure accuracy of the derived K_d value.

Scheme 1



(d) Titration of Zn²⁺ Binding by Absorption Spectroscopy (K_{d2}). A 3.0-mL solution containing 10 μ M Zinpyr-1 in PIPES buffer (100 mM KCl, 50 mM PIPES, pH 7) was prepared, and an initial absorption measurement was made. A portion of Zn²⁺ was added from standardized stock solutions to give an equimolar solution of ligand and metal ion, and the absorbance was measured. Additional Zn²⁺ aliquots were added to give final metal ion concentrations of 250 and 500 μ M and 1, 5, 10, and 15 mM. Calculation of the ΔA by subtracting the 10 μ M Zn²⁺ spectrum from the higher concentration spectra, followed by plotting against wavelength, revealed maximum changes at 497 (increase) and 520 (decrease) nm.

For Zinpyr-2, a 3.0-mL solution containing 19 μ M Zinpyr-2 in PIPES buffer, pH 7 (100 mM KCl, 50 mM PIPES) was prepared, and an initial absorbance measurement was made. Zn²⁺ aliquots were titrated into the solutions to give final concentrations of 1–20 μ M (1 μ M increments), 30, 40, 50, 150, 250, 500, and 750 μ M, and the absorption spectra were recorded. The ΔA values were calculated by subtracting the 0 μ M spectrum from the subsequent spectra and were plotted against the wavelength. The maximum absorption changes occurred at 486 nm (increases) and 508 nm (decreases). The change at 508 nm corresponds to the first binding event, but the increase at 486 nm is not indicative of a single process.

The measurements were repeated at pH 7.5 in HEPES buffer (100 mM KCl, 50 mM HEPES) for both Zinpyr-1 and Zinpyr-2 using the methods described above. The absorbance change for Zinpyr-1 was fit to a binding curve, and the spectral response of Zinpyr-2 was corrected for dilution and analyzed using SPECFIT, a nonlinear least-squares fitting program.⁴⁹

Cell Preparation. COS-7 cells were plated onto ethanol-washed, UV-sterilized glass coverslips and grown to 60–80% confluence at 37 °C in DMEM (Gibco catalog no. 31600-075) supplemented with 10% v/v fetal bovine serum. For labeling, the cells were washed once with HBSS (Gibco catalog no. 11201-092) supplemented with 2 g/L D-glucose and 20 mM HEPES pH 7.4, then incubated with 5 μ M fluorophore in HBSS at 37 °C for 0.5–1 h. Prior to imaging, the labeling solution was aspirated and the cells were washed three times with HBSS.

Cell Imaging. Cells were imaged on a Zeiss Axiovert microscope equipped with a cooled CCD camera (Princeton Instruments, Trenton, NJ). Excitation light was provided by a 150 W Xe arc lamp transmitted through a 465–495-nm excitation filter and a 505-nm long-pass dichroic mirror, and fluorescence was measured after passage through a 513–558-nm emission filter. Filters were obtained from Omega Optical and Chroma Technologies (Brattleboro, VT).

Results and Discussion

Synthesis. The synthesis of Zinpyr-1 was accomplished by a Mannich reaction between bis(2-pyridylmethyl)amine (dipicolylamine or DPA), prepared from 2-pyridinecarboxaldehyde and 2-aminomethylpyridine according to published procedures,⁴² and 2',7'-dichlorofluorescein (DCF, Scheme 1). Formation of the imminium cation by condensation of paraformaldehyde and DPA and subsequent reaction with DCF afforded the desired

compound in ~60% yield after trituration with boiling ethanol and washing with cold water. The crude material, which is >90% pure after trituration (¹H NMR), can be further purified by chromatography on neutral alumina or reverse-phase silica to give analytically pure material (HPLC). This synthesis provides easy access to gram quantities of the desired Zn²⁺ probe.

Although fluorescein undergoes electrophilic substitution preferentially at the 4' and 5' positions,^{50,51} a mixture of structural isomers with substitution at the 4', 5', 2', and 7' positions is obtained when the compound is subjected to the Mannich conditions that were used to prepare Zinpyr-1. These isomers are inseparable by conventional flash chromatography. We therefore envisioned that a fluorescein compound functionalized at the 4' and 5' positions with a synthetically useful group such as an aldehyde could be employed as a scaffold for preparing both the Zinpyr-1 analogue and a variety of related sensors. Scheme 2 outlines the 4-step synthetic route devised to prepare Zinpyr-2 in which the dialdehyde **3** is a key intermediate.

The synthesis of **1** was achieved by modification of the published procedure that involves installation of benzoate protecting groups on the phenolic oxygen of 4',5'-dimethylfluorescein.⁵² In the initial report, **1** was prepared using benzoyl chloride and characterized only by its melting point. Unprotected fluoresceins are highly polar compounds that are only slightly soluble in most common organic solvents. The benzoate protecting groups provide a convenient method for purifying fluorescein compounds by chromatography or crystallization and facilitating subsequent chemical manipulation by enhancing their solubility in organic media. In addition, protecting the phenolic oxygen atoms forces the fluorescein to adopt the lactoid isomer, preventing isomerization between the quinoid and lactoid forms.

Compound **2** can be formed in multigram quantities by bromination of **1** under free radical conditions. The reaction proceeded under facile conditions to give **2** in ~95% purity before recrystallization. No dibromination was observed. Compound **2** can be carried on without purification to the next step, or recrystallized to give highly pure material (+99%, TLC/¹H NMR). Attempts to prepare sensors directly from **2** by direct displacement of the bromides were unsuccessful. Side reactions involving the benzoate protecting groups and lactone ring are suspected to be the problems.

Oxidation of **2** with DMSO in the presence of NaHCO₃ yielded the dialdehyde **3**. Rigorous drying of the DMSO by distillation from CaH₂ followed by storage over molecular sieves is required to obtain the product in ~40% yield. Reactions using undistilled DMSO reduced the isolated yields by >50%. The

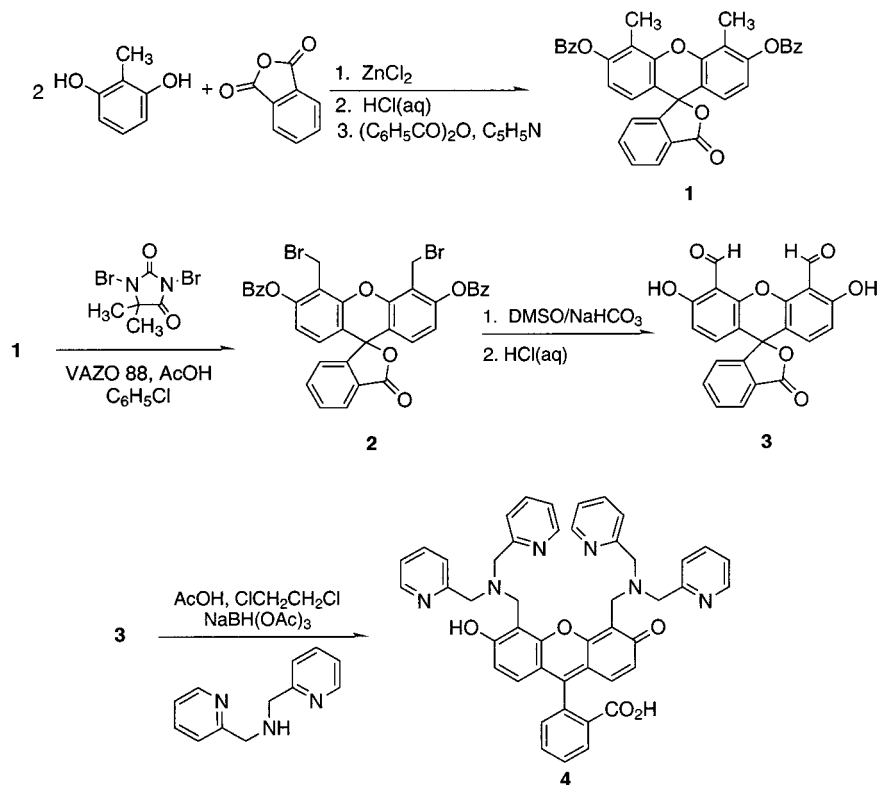
(50) Sandin, R. B.; Orvis, R. L. *J. Org. Chem.* **1958**, *23*, 1234–1235.

(51) Shipchandler, M. T.; Fino, J. R. *Anal. Biochem.* **1986**, *154*, 476–477.

(52) Burton, H.; Kurzer, F. *J. Soc. Chem. Ind. London* **1948**, *67*, 345.

(49) Binstead, R.; Zuberbuhler, A. D. *SPECFIT Global Analysis System*, 2.10 ed.; Spectrum Software Associates: Chapel Hill, NC 27515, 1998.

Scheme 2



synthesis of **3** resulted in cleavage of the benzoate protecting groups, but H-bonding between the phenolic hydrogens and the aldehyde carbonyl oxygens enforces the lactoid isomer, as shown by the NMR chemical shift of the phenolic hydrogen atoms ($\delta = 12.2$), compensating for the loss of the protecting groups. Compound **3** can be condensed with primary amines to give imines, or it can be aminated under reducing conditions to give amines. The synthetic chemistry of **3** and the use of the compound as a scaffold for sensors as well as for other purposes will be the subjects of future reports. Zinpyr-2 was prepared by the reaction of **3** with DPA using NaBH(OAc)₃ as the reducing agent in fairly good yield. The zinc complex of Zinpyr-1 crystallizes within 2 h from an aqueous solution of CH₃CN in the presence of excess NaClO₄. The orange crystalline compound is nonfluorescent under UV light.

Fluorescence Properties of Zinpyr Sensors. Under simulated physiological conditions (50 mM PIPES, 100 mM KCl) at pH 7 in the presence of EDTA to scavenge adventitious metal ions, Zinpyr-1 and Zinpyr-2 have quantum yields of 0.38 and 0.25, respectively. The quantum yields increase to 0.87 for Zinpyr-1 and 0.92 for Zinpyr-2 in the presence of 25 μ M Zn²⁺. The excitation maximum of Zinpyr-1 shifts from 515 nm ($\epsilon = 79.5 \times 10^3 \text{ M}^{-1} \text{ cm}^{-1}$) to 507 nm ($\epsilon = 84.0 \times 10^3 \text{ M}^{-1} \text{ cm}^{-1}$) upon Zn²⁺ complexation. Zinpyr-2 exhibits a similar shift from 498 nm ($\epsilon = 36.8 \times 10^3 \text{ M}^{-1} \text{ cm}^{-1}$) to 490 nm ($\epsilon = 44.9 \times 10^3 \text{ M}^{-1} \text{ cm}^{-1}$) after the addition of Zn²⁺. The slight hypsochromic shift in the absorption wavelength is indicative of coordination of the donor group (phenol) to Zn²⁺.⁵³ Since the phenol is incorporated into the π -system of the fluorophore, coordination to a metal is expected to perturb the electronic structure of the system and produce a shift in the excitation wavelength. The fluorescence response is Zn²⁺-selective. Ca²⁺ and Mg²⁺ concentrations as high as 5 mM produce no change,

and other first-row transition metal ions including Cu⁺, Cu²⁺, Ni²⁺, Co²⁺, Fe²⁺, and Mn²⁺ quench the fluorescence.⁵⁴

The fluorescent increase and binding affinity for Zn²⁺ were characterized by using a dual-metal single-ligand buffer system⁵⁵ comprising 1 mM EDTA, 2 mM Ca²⁺ and 0–1 mM total Zn²⁺. The formation of the [Zn(EDTA)]²⁻ complex, which has an apparent K_d of 2.11 nM under these conditions, allowed the controlled variation of [Zn²⁺]. Figure 2a,b shows the results of representative titrations for Zinpyr-1 and Zinpyr-2, respectively. Whereas the quantum yield of Zinpyr-1 increased by 2.25-fold, changes in the absorption properties of the bound and unbound probe afforded a 3.1-fold change in integrated emission. Similarly, the quantum yield of Zinpyr-2 increased by \sim 3.7-fold, and the integrated emission increased 6.0-fold.

The Zn²⁺ affinity of the Zinpyr sensors was determined by performing these measurements in triplicate using different Ca²⁺/EDTA/Zn²⁺ buffers. The measurements indicated that the [(Zn)/Zinpyr-2] complex has an apparent K_d at pH 7.0 of 0.5 ± 0.1 nM (mean \pm esd) that is slightly lower than that of Zinpyr-1, for which the K_d is 0.7 ± 0.1 nM. The [Zn(DPA)]²⁺ complex has an apparent K_d of 70 nM at pH 7, approximately 2 orders of magnitude weaker than the observed K_d values for the Zinpyr compounds.⁵⁶ The tighter binding of the latter suggests that there are additional groups involved in Zn²⁺ chelation. The fluorescence response fit to a Hill coefficient of 1, consistent with the formation of a 1:1 Zinpyr:Zn²⁺ complex responsible for the enhancement. The initial speculation that Zinpyr-1 might bind Zn²⁺ in a "TPEN-like" manner, where TPEN is the intracellular heavy metal ion chelator *N,N,N',N'*-tetra(2-picolyl)ethylenediamine, was not consistent with the shifting of the excitation wavelengths or the binding affinity of TPEN (\sim 1 fM at pH 7).

(54) Details provided in Supporting Information.

(55) Wolf, H. U. *Experientia* **1973**, *29*, 241–249.

(56) Anderegg, G.; Hubmann, E.; Podder, N. G.; Wenk, F. *Helv. Chim. Acta* **1977**, *60*, 123–140.

(53) Balzani, V.; Scandola, F. *Supramolecular Photochemistry*; Ellis Horwood: New York, 1991.

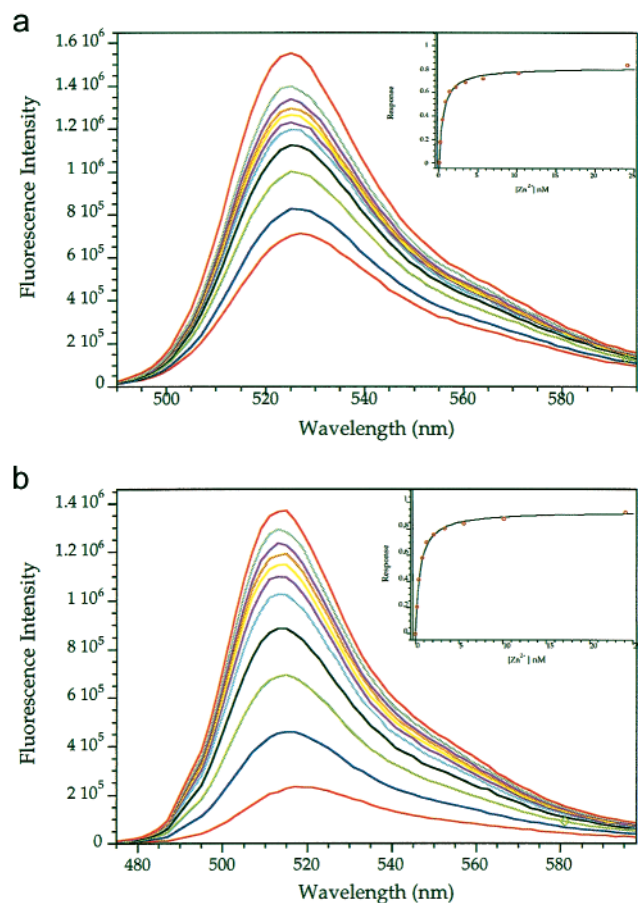


Figure 2. Fluorescence emission response of Zinpyr-1 (a) and Zinpyr-2 (b) to buffered Zn²⁺ solutions. Spectra were acquired in 100 mM KCl, 50 mM PIPES, pH 7.00, at 25 °C. Excitation was provided at 490 nm with 0.25-mm slit widths. Emission data were corrected for the response of the detector using the manufacturer-supplied curve, and the emission data points at 490 nm, which were perturbed by scatter, have been removed for clarity. The spectra shown are for free zinc buffered at 0, 0.172, 0.424, 0.787, 1.32, 2.11, 3.34, 5.60, 10.2, and 24.1 nM, respectively. For the final spectrum (containing 1 mM EDTA and 1 mM Zn²⁺), additional ZnCl₂ was added to provide ~25 μM free Zn²⁺. Inset: fluorescence response obtained by integrating the emission spectra between 500 and 575 nm, subtracting the baseline (0 Zn²⁺) spectrum and normalizing to the full scale response (25 μM free Zn²⁺).

The fluorescence of Zinpyr was also enhanced by protonation of the tertiary amines. Zinpyr fluorescence is almost completely quenched at pH > 12, and reaches a maximum for both sensors near pH 5.5. The pH change fits to an apparent pK_a of 8.4 for Zinpyr-1 (Figure 3a) and 9.4 for Zinpyr-2 (Figure 3b). The plateau of the fluorescence corresponds to a state of the molecule in which both tertiary amines are protonated. The difference in the pK_a values between the two sensors can be attributed to the chlorine atoms on the xanthenone ring, which decrease the pK_a of the phenols. The increased acidity of the phenol groups should have an effect on the fluorescence pK_a by modifying the local pH in the vicinity of the amines. In addition to the observed difference in pK_a values for the two sensors, each of the tertiary amines of the individual molecules is predicted to have a different pK_a value because of the difference in environments between the amines on the phenolic and keto oxygen halves of the molecule. This difference is not manifest in a stepwise change in the fluorescence intensity; however, the amine adjacent to the keto oxygen should become protonated before the more acidic site adjacent to the deprotonated phenol. The fluorescence quenching observed for both molecules below pH

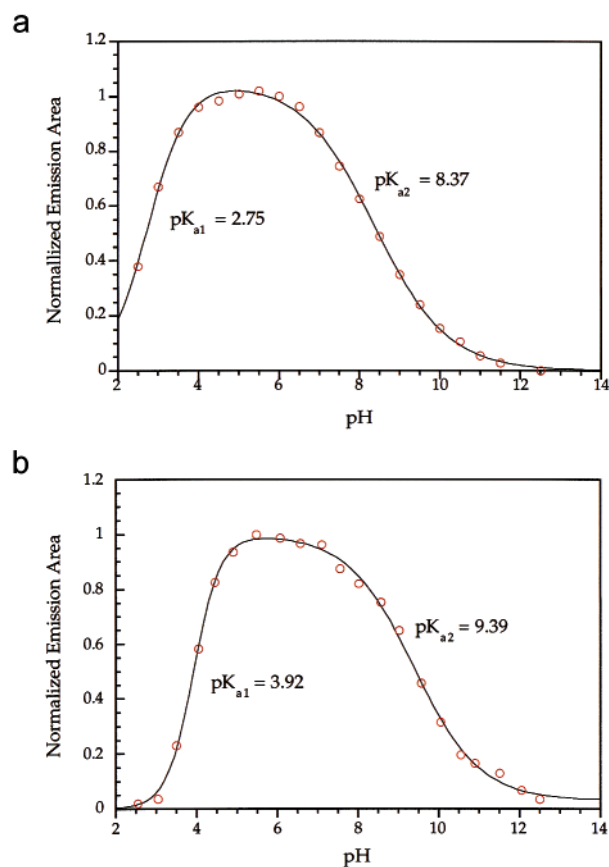


Figure 3. Plot of the normalized integrated emission intensity versus pH for Zinpyr-1 (a) and Zinpyr-2 (b). The increase in fluorescence corresponds to protonation of both tertiary amines, and the decrease corresponds to the isomerization of the fluorescein to its nonfluorescent zwitterion isomer. The emission intensity varies only minimally from the physiological range, which is an important property for measuring intracellular [Zn²⁺] changes.

5.5, with a pK_a of 2.8 for Zinpyr-1 and 3.9 for Zinpyr-2, is attributed to the formation of the nonfluorescent diphenolic zwitterion isomer.⁵⁷

At high pH, because the unbound sensor is more efficiently quenched, the magnitude of Zn²⁺-induced fluorescence change is more dramatic, increasing over 200-fold at pH 12. The quenching of the fluorophore at high pH and enhancement by H⁺ and Zn²⁺ are consistent with a photoinduced electron transfer (PET) mechanism from the benzylic amines. Inhibition of PET by coordination of d¹⁰ transition metals or protons to amines is commonly observed mechanism for fluorescent enhancement.^{23,34} The observed fluorescence increase with Cd²⁺ also supports the validity of this suggested mechanism. Although the fluorescence of the Zinpyr sensors is enhanced by protons as well as Zn²⁺, the quantum yield experiment demonstrates that the emission intensity of the protonated form is significantly lower than that of the Zn complex. More importantly, the emission intensity over the physiologically relevant pH range (pH 5.5 to pH 8) does not vary significantly (Figure 3), so Zn²⁺-induced changes can be readily measured.

Stoichiometry, K₄₂, and Solution Behavior. Small increases in the absorption spectrum of Zinpyr-1 can be observed by titrating more than 1 equivalent of Zn²⁺ per ligand into buffered solutions of Zinpyr-1 at pH 7. At Zn²⁺ concentrations in the micromolar-to-millimolar range, spectral changes occur with maxima at 497 nm (increases) and 520 (decreases) (Figure 4).

(57) Makuszewski, R.; Diehl, H. *Talanta* **1980**, *27*, 937–46.

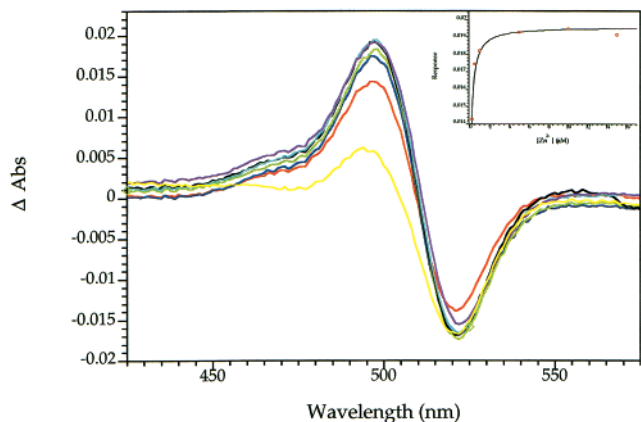


Figure 4. Plot of the difference in absorption between the 1:1 Zinpyr-1: Zn^{2+} spectrum, and the absorption spectra after the addition of Zn^{2+} to give concentrations of 250 and 500 μM and 1, 5, 10, and 15 mM. Inset: plot of the change in absorbance and the concentration of $[\text{Zn}^{2+}]$.

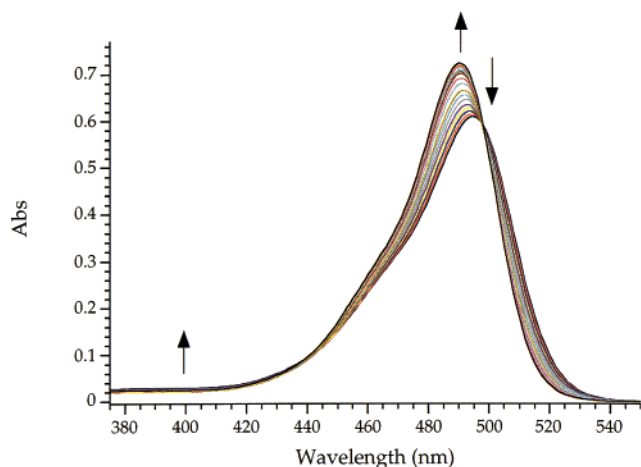


Figure 5. Absorption spectra of Zinpyr-2 [19 μM] after the addition of Zn^{2+} to give final concentrations of 8–20 by increments of 1, 30, 40, 50, 150, 250, 500, and 750 μM . Addition of Zn^{2+} induces a decrease and absorption at 508 nm and an increase at 486 nm.

Examination of the absorption changes suggested the occurrence of a second binding event with a weak K_{d2} in the vicinity of $\sim 85 \pm 10 \mu\text{M}$. The affinity of this weaker binding event K_{d2} increased to $\sim 35 \mu\text{M}$ at pH 7.5, consistent with the second Zn^{2+} binding associated with displacement of a single proton.

The binding of Zn^{2+} by Zinpyr-2 was accompanied by slightly different changes in the absorption spectra (Figure 5). Titration through the first binding event showed that the absorption changes around 485 indicate the occurrence of more than one process. Addition of greater than one equivalent of Zn^{2+} produced small changes in the absorption spectra of Zinpyr-2 similar to the behavior of Zinpyr-1. Analysis of the spectral data with SPECFIT suggest a K_{d2} in the range of $9.0 \pm 1.0 \mu\text{M}$, which decreases to $\sim 2 \mu\text{M}$ at pH 7.5. Figure 6 shows the percentage of each species that was detected during the titration of Zinpyr-2 (19 μM) with increasing concentrations of total Zn^{2+} . The second binding event for both ligands was not associated with a measurable change in fluorescence at physiologically relevant pH. Formation of insoluble zinc(II) hydroxide species at high $[\text{Zn}^{2+}]$ and pH 7 makes it difficult to estimate free metal ion concentrations, so the values reported apply only to the stated conditions. These experiments suggest, however, that the affinity of the second binding site for Zn^{2+} is several

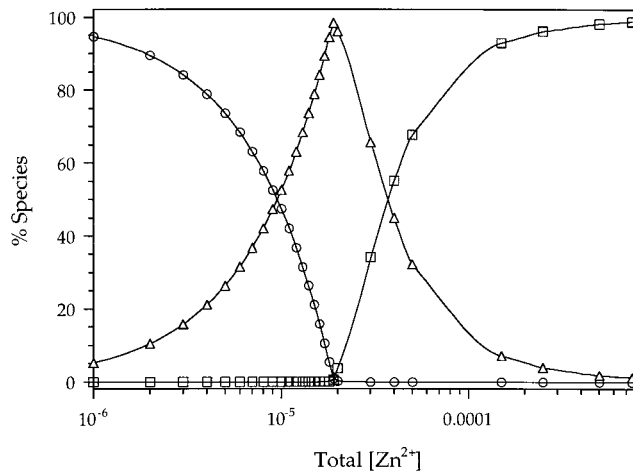


Figure 6. Plot of the percentage of each species present in the titration of Zinpyr-2 with increasing concentrations of Zn^{2+} . The titration was performed with 19 μM Zinpyr-2 in PIPES buffer (pH 7, 100 mM KCl). The total $[\text{Zn}^{2+}]$ represents the total concentration of Zn^{2+} titrated into the solution. Zinpyr-2 (O) decreases upon the formation of the $[(\text{Zn})\text{-Zinpyr-2}]$ complex (Δ). At higher concentrations of Zn^{2+} , $[(\text{Zn})_2\text{Zinpyr-2}]^{2+}$ (\square) forms. The formation of $[(\text{Zn})_2\text{Zinpyr-2}]^{2+}$ is not detected until all of the higher-affinity 1/1 sites are occupied.

orders of magnitude weaker than the first and is not accompanied by a fluorescence change at pH 7.

Scheme 3 shows our interpretation of the behavior of the Zinpyr ligands in solution, which is consistent with all of the spectral measurements. At pH 7, both benzylic amines are expected to be largely protonated, inhibiting PET quenching of the unmetallated fluorophore. Binding of the first Zn^{2+} more efficiently interrupts the PET process and increases the HOMO–LUMO gap between the S_0 and S_1 energy levels. The K_{d1} value is lower than that of DPA because of additional coordination by the phenolic oxygen. It is difficult to measure accurately the affinity of the second binding event, because Zn^{2+} is added from unbuffered solutions, and the Zn^{2+} ion has limited solubility at pH 7–7.5; however, a second binding event is consistent with all of our observations, including the X-ray crystal structure determination. The measured K_{d2} of both ligands is significantly weaker than K_{d1} , presumably because of loss of coordination by the phenol and electrostatic repulsion between the positively charged metallated ligand and the incoming Zn^{2+} cation. The lack of a significant shift in the absorbance, and the persistence of a fluorescent signal at high concentrations of Zn^{2+} , suggest that the lactone ring remains open in aqueous solution.

Structural Studies. The nature of the Zn^{2+} complex of Zinpyr-1 in the solid state was investigated by X-ray crystallography. Attempts to crystallize **6** with Cl^- , I^- , NO_3^- , PF_6^- , BF_4^- , BPh_4^- , CF_3SO_3^- and SO_4^{2-} counterions in a variety of solvents failed to yield X-ray quality crystals. Only the ClO_4^- complex yielded single crystals of suitable quality for structural analysis. The structure of **6** is displayed in Figure 1 as an ORTEP diagram. Single-crystal X-ray diffraction results are shown in Table 1, and selected bond distances and angles are furnished in Table 2. Two ClO_4^- and six disordered H_2O molecules are also present in the asymmetric unit. The structure of **6** is, to our knowledge, the first X-ray structure of a metal bound to fluorescein molecule having appended donor moieties. A survey of the CSD (Cambridge Structural Database)⁵⁸ revealed only nine examples of crystal structures of any

(58) Allen, F. H.; Kennard, O. *Chemical Design Automation News*, **1993**, 8, 31–37.

Scheme 3

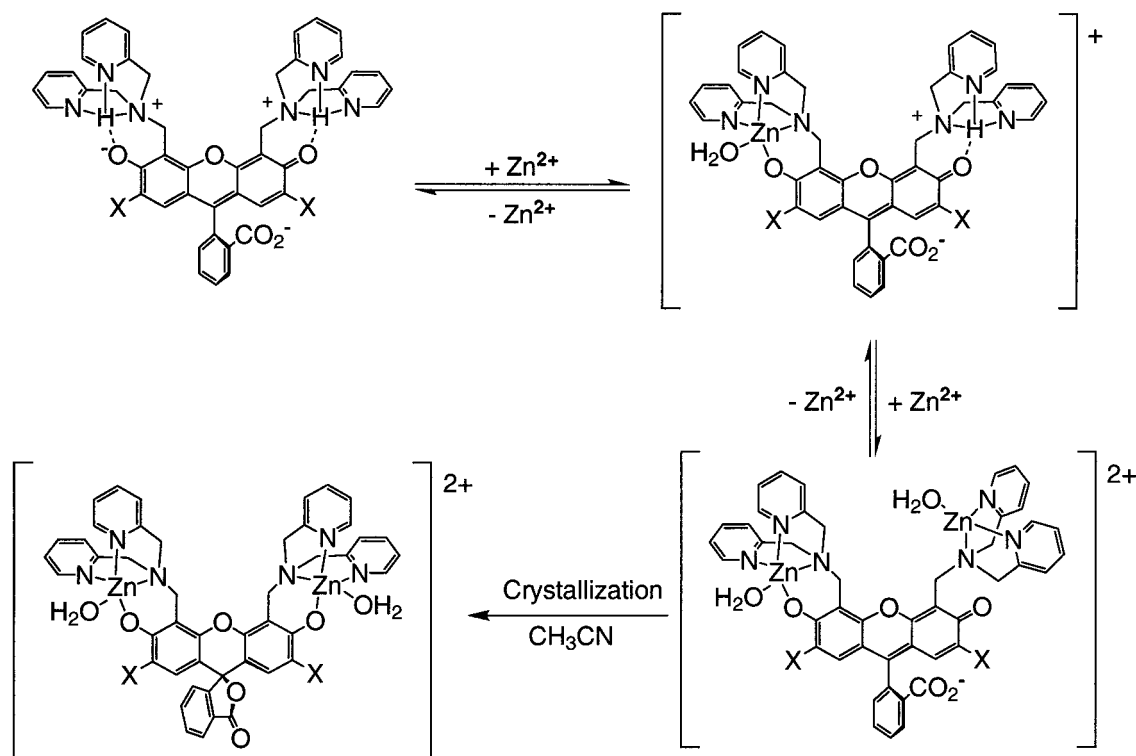


Table 2. Selected Interatomic Distances (Å) and Angles (deg) for [Zn₂(Zinpyr-1)(H₂O)₂](ClO₄)₂·6H₂O (6·6H₂O)^a

Bond Lengths		Bond Angles	
Zn(1)–O(3)	1.942(6)	N(1)–Zn(1)–O(6)	170.0(3)
Zn(1)–O(6)	2.043(6)	N(1)–Zn(1)–N(2)	79.9(3)
Zn(1)–N(1)	2.178(7)	O(3)–Zn(1)–O(6)	97.4(2)
Zn(1)–N(2)	2.086(8)	N(2)–Zn(1)–N(3)	115.4(3)
Zn(1)–N(3)	2.072(8)	N(3)–Zn(1)–O(3)	119.7(3)
		O(3)–Zn(1)–N(2)	121.4(3)
Zn(2)–O(5)	1.954(6)	N(4)–Zn(2)–O(7)	171.5(3)
Zn(2)–O(7)	2.046(6)	N(4)–Zn(2)–N(5)	79.5(3)
Zn(2)–N(4)	2.178(7)	O(5)–Zn(2)–O(7)	94.6(3)
Zn(2)–N(5)	2.087(8)	N(5)–Zn(2)–N(6)	124.4(3)
Zn(2)–N(6)	2.086(8)	N(6)–Zn(2)–O(5)	110.6(3)
		O(5)–Zn(2)–N(5)	121.5(3)

^a Numbers in parentheses are estimated standard deviations in the last digit(s). Atom labels are provided in Figure 1.

fluorescein-based molecules and only one metal complex, that of Pb²⁺. The relatively few examples of fluorescein crystal structures have been attributed to properties of the molecule that disfavor crystallization.⁵⁹

The Zn²⁺ centers in [Zn₂(Zinpyr-1)(H₂O)₂](ClO₄)₂·6H₂O are trigonal bipyramidal, a relatively common coordination geometry for this metal ion. Each Zn²⁺ ion is coordinated by the three nitrogen atoms of one DPA arm, a phenolic oxygen atom, and a water molecule. The tertiary amine atom and water molecule occupy the axial positions, with the pyridine and phenol oxygen atoms in the equatorial sites. The bond lengths and angles are similar to those in X-ray structures of zinc complexes of similar tripodal N₃O ligands.⁶⁰ The fluorescein fragment adopts the lactoid form, which is consistent with the lack of fluorescence of the orange crystals under UV light. Since the complex fluoresces in solution, we conclude that crystallization induces formation of the lactone.

(59) Tremayne, M.; Kariuki, B. M.; Harris, K. D. M. *Angew. Chem., Int. Ed. Engl.* **1997**, *36*, 770–772.

(60) Troesch, A.; Vahrenkamp, H. *Eur. J. Inorg. Chem.* **1998**, 827–832.

Attempts to crystallize a 1:1 ligand:metal complex were unsuccessful. Reactions of Zinpyr-1 in the presence of <1 equiv of Zn²⁺ afforded only the 2:1 complex. Complexation of Zn²⁺ in the first binding site leaves a DPA arm uncoordinated, and the resultant multiple degrees of freedom might disfavor crystallization. The 2:1 complex is significantly more symmetric and rigid, leading to more favorable crystal packing opportunities.

Formation of mixed complexes with partially coordinated Zn²⁺ is one of the perceived shortcomings of the quinoline-based sensors. Coordination of Zn²⁺ by the ligand arm of the Zinpyr sensor leaves one open coordination site that is occupied by a water molecule in the crystal structure. Although this open coordination site offers the possibility to form mixed complexes, binding at this open site should be relatively weak, because the coordination sphere of the Zn²⁺ metal ion is nearly saturated. The open site is also fairly crowded, which should hinder coordination of macromolecular ligands.

Intracellular Staining with Zinpyr-1 and Zinpyr-2. Incubation of Cos-7 cells with 5 μM Zinpyr reagent produced bright punctate staining patterns similar to observations made with quinoline-based sensors.^{5,12} These observations were made with both Zinpyr-1 and Zinpyr-2. The bright fluorescence colocalized with the acidic compartment probe LysoTracker (Molecular Probes, Eugene OR). The initial Zinpyr fluorescence was not diminished by addition of TPEN, which suggests that the concentration of free Zn²⁺ in these cells is lower than the detection limit of the sensor (~0.1 nM). The low free Zn²⁺ may reflect buffering and chelation by exogenous Zinpyr. To draw conclusions about endogenous Zn²⁺, further experiments will be necessary in which the Zinpyr concentration is varied and the observed free [Zn²⁺] extrapolated to zero dye. The fluorescence initially observed is most likely background induced by protonation within vesicular membranes (Figure 7a). The apparent propensity of these molecules to become trapped in acidic compartments represents the principal challenge in the

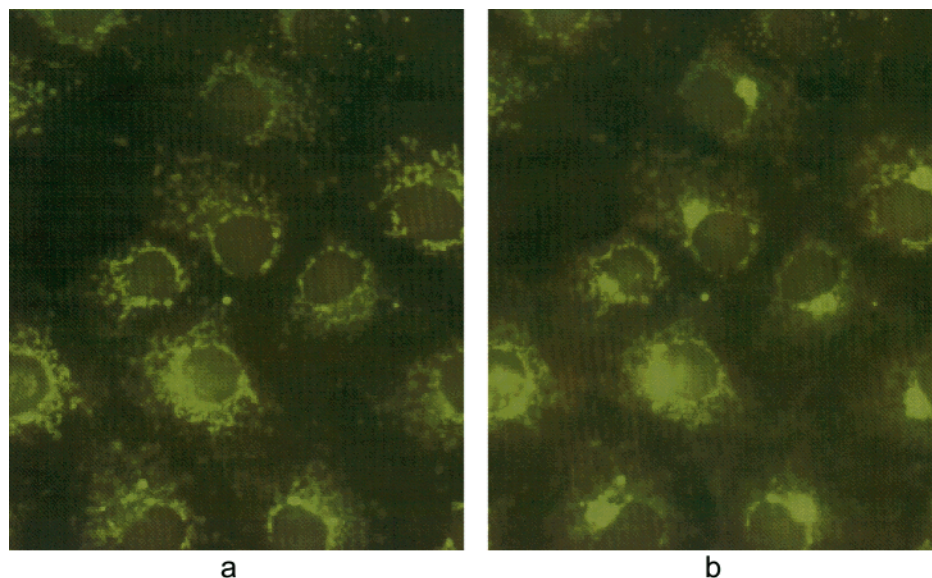


Figure 7. (a) Fluorescence microscopy images of COS-7 cells labeled with 5 μM Zinpyr-1 for 0.5 h at 37 $^{\circ}\text{C}$. The fluorescence is not diminished by the addition of the high-affinity membrane-permeable heavy-metal chelator, TPEN, indicating the fluorescence is not Zn^{2+} -induced. (b) The bright perinuclear punctate staining increases upon the addition of the zinc ionophore Zn^{2+} /pyrithione and can be reversed by treatment with TPEN.

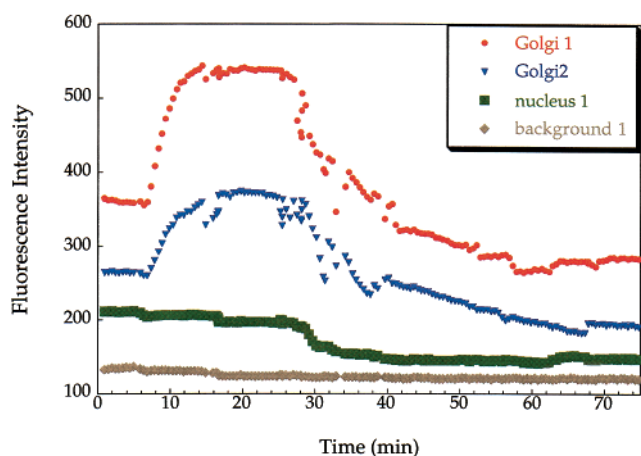


Figure 8. Fluorescence intensity analysis of COS-7 cells shown in Figure 7. The fluorescence intensity observed for two of the bright perinuclear punctate regions (Golgi), and one nucleus are shown. Exogenous Zn^{2+} was added using the zinc ionophore pyrithione 5 min after the initial treatment with Zinpyr-1, causing a dramatic increase in fluorescence in the puncta. The enhancement was reversed by treatment with TPEN that was added at the 30 min mark. Cytosolic and nuclear regions selected for analysis did not respond to exogenously added Zn^{2+} /pyrithione or TPEN.

measurement of Zn^{2+} within cells using Zinpyr sensors. The nature of the fluorescence staining suggested that the sensor localized in a specific cell organelle. Additional double-labeling experiments with a galactosyl transferase-enhanced cyan fluorescent protein fusion (GT-ECFP) that colocalizes in the medial/trans-Golgi revealed that Zinpyr stains the Golgi or a Golgi-associated vesicle.⁴⁰

A significant enhancement of the fluorescence in the puncta could be observed when the cells were treated with exogenous Zn^{2+} (50 μM) using the zinc ionophore pyrithione (2-mercapto-pyridine *N*-oxide, 20 μM , Figure 7b). Addition of TPEN (100 μM) reversed the fluorescence in the organelles to levels observed before the treatment with Zn^{2+} (Figure 8). Although the background fluorescence from the unmetallated sensor presents a significant difficulty in measuring the free $[\text{Zn}^{2+}]$,

monitoring the $[\text{Zn}^{2+}]$ change is straightforward and represents a significant application for these sensors. The ability of these probes to image exogenously applied Zn^{2+} demonstrates that Zinpyr sensors can produce a discernible change in the fluorescence signal even though the unmetallated/protonated sensor has a relatively bright fluorescence. Examination of cell types that undergo fluctuations in endogenous $[\text{Zn}^{2+}]$ as a result of biochemical events would be of interest.

Conclusions

We have developed two new fluorescent Zn^{2+} sensors, Zinpyr-1 (**5**) and Zinpyr-2 (**4**), utilizing fluorescein as the reporting group. These new sensors are amenable to intracellular studies as a result of their favorable optical properties, binding affinity, water solubility, and their ability to be loaded passively into cells. The primary shortcoming of the Zinpyr sensors is their sensitivity to protons and the relatively modest fluorescence enhancement upon binding of the analyte. Access to the fluorescein dialdehyde (**3**), the key intermediate in the synthesis of Zinpyr-2, is significant because it can be utilized as a starting point for the design of future sensors. In addition to sensor design, the aldehyde functionality of **3** provides a convenient synthetic means for introducing a fluorescein molecule passively into a variety of systems. The ability to modify synthetically commercially available substituted fluorescein compounds such as fluorescein amine is often limited because the compounds are relatively unreactive, and require harsh conditions for introduction into the desired system.

The Zinpyr dyes are the first generation of molecules in an ongoing effort to develop Zn^{2+} sensors for the neurosciences. Our current efforts are focused on preparation of sensors that are completely quenched in the absence of Zn^{2+} and on developing a series of probes with a range of binding affinities to study free Zn^{2+} at the different concentrations proposed to be present in living systems. The use and elaboration of the synthetic methodologies developed here to prepare the dialdehyde **3** are key steps in accomplishing these goals. In addition to new sensors, we are also continuing to apply the Zinpyr sensors to investigating the roles of free Zn^{2+} in neurophysiology.

Acknowledgment. This work was supported at MIT by seed funds to launch new projects in the neurosciences and more recently by a grant from the McKnight Foundation for the Neurosciences. The NMR spectrometer at the MIT DCIF was purchased with support from the National Science Foundation under grant no. CHE9808061. S.C.B. and S.J.L. thank J. Du Bois, K. J. Franz, D. A. Kopp, G. T. Gassner, and W. M. Davis for helpful suggestions. S.C.B. thanks R. A. Binstead of Spectrum Software Associates for assistance with SPECFIT. B.S. was supported by the Swiss National Science Foundation as a postdoctoral fellow. G.K.W. and R.Y.T. thank Dr. J. Llopis for initial assistance with the GT-ECFP labeling experiments.

The award of a NIH training grant to support G.K.W. (GM19804-02) is gratefully acknowledged.

Supporting Information Available: Experimental methods for metal ion selectivity experiments; Figures S1 and S2 showing the fluorescence response of Zinpyr-1 and Zinpyr-2 to various divalent metal ions; Figures S3-S7 showing the ¹H NMR spectra of compounds **1-5**; Figure S8 showing the fully labeled ORTEP diagram; and Tables S1-S4 showing pertinent crystallographic information for [Zn₂(Zinpyr-1)(H₂O)₂](ClO₄)₂·6H₂O.

JA010059L